



Citation for published version:

Bloschl, G, Hall, J, Kjeldsen, T & Macdonald, N 2019, 'Changing climate both increases and decreases European river floods', *Nature*, vol. 573, pp. 108-111. <https://doi.org/10.1038/s41586-019-1495-6>

DOI:

[10.1038/s41586-019-1495-6](https://doi.org/10.1038/s41586-019-1495-6)

Publication date:

2019

Document Version

Peer reviewed version

[Link to publication](#)

This is a post-peer-review, pre-copyedit version of an article published in *Nature*. The final authenticated version is available online at: <https://doi.org/10.1038/s41586-019-1495-6>

University of Bath

General rights

Copyright and moral rights for the publications made accessible in the public portal are retained by the authors and/or other copyright owners and it is a condition of accessing publications that users recognise and abide by the legal requirements associated with these rights.

Take down policy

If you believe that this document breaches copyright please contact us providing details, and we will remove access to the work immediately and investigate your claim.

Changing climate both increases and decreases European river floods

Günter Blöschl^{1†}, Julia Hall^{1†}, Alberto Viglione^{1, 12}, Rui A. P. Perdigão¹, Juraj Parajka¹, Bruno Merz², David Lun¹, Berit Arheimer³, Giuseppe T. Aronica⁴, Ardian Bilibashi⁵, Miloň Boháč⁶, Ognjen Bonacci⁷, Marco Borga⁸, Ivan Čanjevac⁹, Attilio Castellarin¹⁰, Giovanni B. Chirico¹¹, Pierluigi Claps¹², Natalia Frolova¹³, Daniele Ganora¹², Liudmyla Gorbachova¹⁴, Ali Gül¹⁵, Jamie Hannaford¹⁶, Shaun Harrigan¹⁷, Maria Kireeva¹³, Andrea Kiss¹, Thomas R. Kjeldsen¹⁸, Silvia Kohnová¹⁹, Jarkko J. Koskela²⁰, Ondrej Ledvinka⁶, Neil Macdonald²¹, Maria Mavrova-Guirguinova²², Luis Mediero²³, Ralf Merz²⁴, Peter Molnar²⁵, Alberto Montanari⁹, Conor Murphy²⁶, Marzena Osuch²⁷, Valeryia Ovcharuk²⁸, Ivan Radevski²⁹, José L. Salinas¹, Eric Sauquet³⁰, Mojca Šraj³¹, Jan Szolgay¹⁸, Elena Volpi³², Donna Wilson³³, Klodian Zaimi³⁴, and Nenad Živković³⁵

¹Institute of Hydraulic Engineering and Water Resources Management, Technische Universität Wien, Vienna, Austria

²Helmholtz Centre Potsdam, GFZ German Research Centre for Geosciences, Potsdam, Germany

³Swedish Meteorological and Hydrological Institute, Norrköping, Sweden

⁴Department of Engineering, University of Messina, Messina, Italy

⁵CSE – Control Systems Engineer, Renewable Energy Systems & Technology, Tirana, Albania

⁶Czech Hydrometeorological Institute, Prague, Czechia

⁷Faculty of Civil Engineering, Architecture and Geodesy, Split University, Split, Croatia

⁸Department of Land, Environment, Agriculture and Forestry, University of Padova, Padua, Italy

⁹University of Zagreb, Faculty of Science, Department of Geography, Zagreb, Croatia

¹⁰Department of Civil, Chemical, Environmental and Materials Engineering (DICAM), Università di Bologna, Bologna, Italy

¹¹Department of Agricultural Sciences, University of Naples Federico II, Naples, Italy

¹²Department of Environment, Land and Infrastructure Engineering (DIATI), Politecnico di Torino, Turin, Italy

¹³Department of Land Hydrology, Lomonosov Moscow State University, Moscow, Russia

¹⁴Department of Hydrological Research, Ukrainian Hydrometeorological Institute, Kiev, Ukraine

¹⁵Department of Civil Engineering, Dokuz Eylül University, Izmir, Turkey

¹⁶Centre for Ecology & Hydrology, Wallingford, Oxfordshire, UK

¹⁷Forecast Department, European Centre for Medium-Range Weather Forecasts (ECMWF), UK

¹⁸Department of Architecture and Civil Engineering, University of Bath, Bath, UK

¹⁹Slovak University of Technology in Bratislava, Faculty of Civil Engineering, Department of Land and Water Resources Management, Bratislava, Slovakia

²⁰Finnish Environment Institute, Helsinki, Finland

²¹Department of Geography and Planning & Institute of Risk and Uncertainty, University of Liverpool, Liverpool, UK

²²University of Architecture, Civil Engineering and Geodesy, Sofia, Bulgaria

²³Department of Civil Engineering: Hydraulic, Energy and Environment, Universidad Politécnica de Madrid, Madrid, Spain

²⁴Department for Catchment Hydrology, Helmholtz Centre for Environmental Research – UFZ, Halle, Germany

²⁵Institute of Environmental Engineering, ETH Zurich, Zurich, Switzerland

²⁶Irish Climate Analysis and Research Units (ICARUS), Department of Geography, Maynooth University, Ireland

²⁷Department of Hydrology and Hydrodynamics, Institute of Geophysics Polish Academy of Sciences, Warsaw, Poland

²⁸Hydrometeorological Institute, Odessa State Environmental University, Odessa, Ukraine

²⁹Institute of Geography, Faculty of Natural Sciences and Mathematics, Ss. Cyril and Methodius University, Skopje, Republic of Macedonia

³⁰Irstea, UR RiverLy, Lyon-Villeurbanne, France

³¹University of Ljubljana, Faculty of Civil and Geodetic Engineering, Ljubljana, Slovenia

³²Department of Engineering, University Roma Tre, Rome, Italy

³³Norwegian Water Resources and Energy Directorate, Oslo, Norway

³⁴Institute of Geo-Sciences, Energy, Water and Environment (IGEWE), Polytechnic University of Tirana, Tirana, Albania

³⁵University of Belgrade, Faculty of Geography, Belgrade, Serbia

* e-mail: bloeschl@hydro.tuwien.ac.at

† These authors contributed equally to this work.

1 **Abstract**

2
3 **Climate change has led to concerns of increasing river floods resulting from the greater water**
4 **holding capacity of a warmer atmosphere¹. This concern is reinforced by evidence of increasing**
5 **economic losses in many parts of the world, including Europe². Any changes in river floods**
6 **would have lasting implications for designing flood protection measures and for flood risk**
7 **zoning. Existing studies have been unable to identify a consistent continental-scale climatic**
8 **change signal in flood discharge observations in Europe³, because of limited spatial coverage**
9 **and choices in the grouping of hydrometric stations. Here we show that clear regional patterns**
10 **of both increases and decreases in observed river flood discharges in the last five decades in**
11 **Europe are evident, which are likely manifestations of a changing climate. Our results suggest**
12 **that (i) increasing autumn and winter rainfall has led to increasing floods in northwestern**
13 **Europe, (ii) decreasing precipitation and increasing evaporation have led to decreasing floods**
14 **in medium and large catchments in southern Europe and (iii) decreasing snowcover and**
15 **snowmelt as a result of warmer temperatures have led to decreasing floods in eastern Europe.**
16 **Regional flood discharge trends in Europe range from an increase of +11.4% per decade to a**
17 **decrease of -23.1%. Notwithstanding the spatial and temporal heterogeneity of the**
18 **observational record, the flood changes identified here are broadly consistent with climate**
19 **model projections for the next century^{4,5}, suggesting that climate-driven changes are already**
20 **happening, which supports calls for future climate change consideration in flood risk**
21 **management.**

22

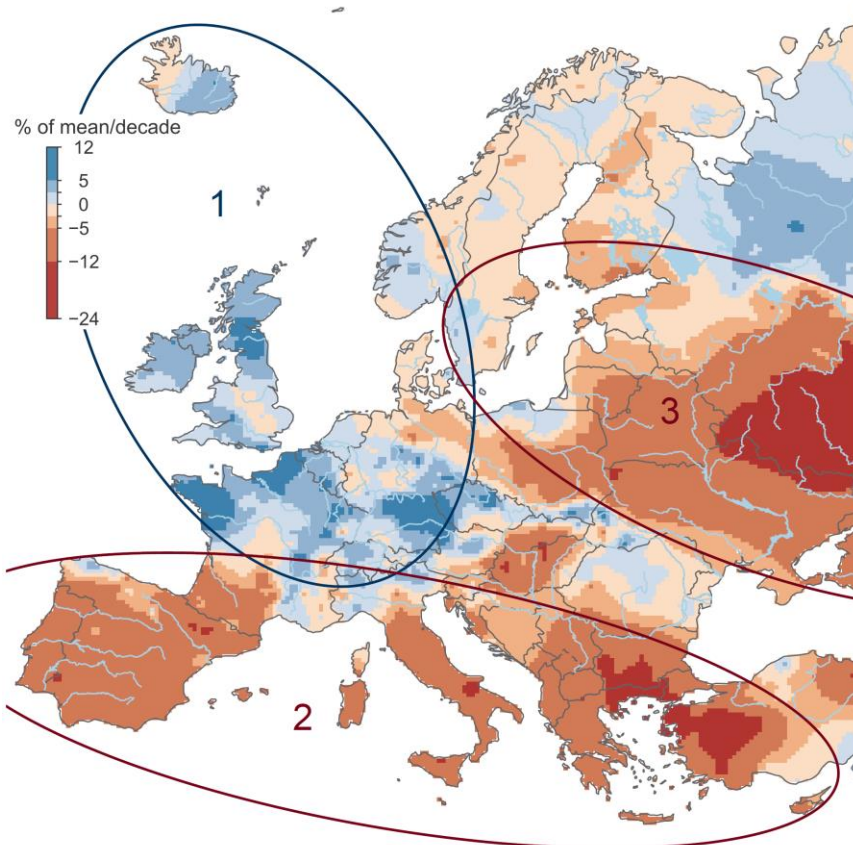
23 River floods are among the most costly natural hazards. Global annual average losses are estimated
24 at US \$104 billion⁶, and are expected to increase as a result of economic growth, urbanization and
25 climatic change^{2,7}. Physical arguments of increased heavy precipitation resulting from the enhanced
26 water holding capacity in a warmer atmosphere and the occurrence of numerous large floods have
27 exacerbated concerns of increasing flood magnitudes¹. However, observations of individual extreme
28 events do not necessarily imply that the long-term statistics of flood discharge are also increasing³.

30 In Europe, a climatic change signal in flood discharges over the past five decades has been
31 demonstrated in relation to changes in timing of floods within the year⁸. For example, in northeastern
32 Europe, warmer air temperatures have led to earlier spring snowmelt floods. However, changes in
33 flood discharges are still contested, as no coherent large-scale observational evidence has to date been
34 available at the continental scale, as a result of limited spatial coverage and choices in the grouping
35 of hydrometric stations³. A number of studies point towards increases in flood discharges in western
36 Europe in the past five decades. The findings include upward trends in flood discharges in 15% of
37 the stations⁹, an increase in the occurrence of extreme flood discharges by 44%¹⁰, and significant
38 increases in major-flood occurrence in medium sized catchments¹¹. However, these studies are not
39 fully representative as the stations are mainly clustered around western Europe.

41 Here we analyze the most comprehensive data set of flood observations in Europe¹² to show that a
42 changing climate has increased river flood discharges in some regions of Europe, but decreased floods
43 in others. We base our analysis on river discharge observations from 3738 gauging stations for the
44 period 1960–2010. The catchment areas range between 5 and 100,000 km². For each station, we
45 extracted a series consisting of the highest peak discharge recorded in each calendar year, the annual
46 maximum peak flow. We estimated the trend in each series using the Theil-Sen slope estimator, tested
47 the statistical significance with the Mann-Kendall test, and estimated regional trends by spatial
48 interpolation. We also derived the long-term evolution of floods using a 10-year moving average filter.
49 Finally, we analyzed in a similar fashion the change signal of three plausible drivers of floods: annual
50 maximum 7-day precipitation; highest monthly soil moisture in each year; and spring (January to
51 April) mean air temperature as a proxy for snowmelt and snowfall-to-rain transition. We examined
52 the consistency of the changes in the drivers with those of the floods by comparing the change patterns
53 and by Spearman rank correlation coefficients.

55 Our data show a clear regional pattern in flood trends across Europe (Fig. 1). Regional trends, relative
56 to the mean flood discharges over 1960-2010, range from an increase of +11.4% to a decrease
57 of -23.1% per decade (Fig. 1). The uncertainties of the regional trends (Extended Data Fig. 2b) are
58 small (typically between 1 and 2% per decade) relative to the spatial signal. Local trends (Extended
59 Data Fig. 2a) at the stations range from an increase of +17.8% to a decrease of -28.8% of the long-
60 term station mean per decade. The spatial patterns of trends are grouped into three main regions. In
61 northwestern Europe (Fig. 1, region 1), ~69% of stations show an increasing flood trend (Extended
62 Data Table 2a) with an average local increase of +2.3% per decade. In southern Europe (Fig. 1, region
63 2), ~74% of stations show a decreasing trend with a regional average trend of -5% per decade. In
64 eastern Europe (Fig. 1, region 3), ~78% of stations show a decreasing flood trend with an average
65 decrease of -6% per decade. In northern Scandinavia and northwestern Russia, trends are less
66 pronounced.

67

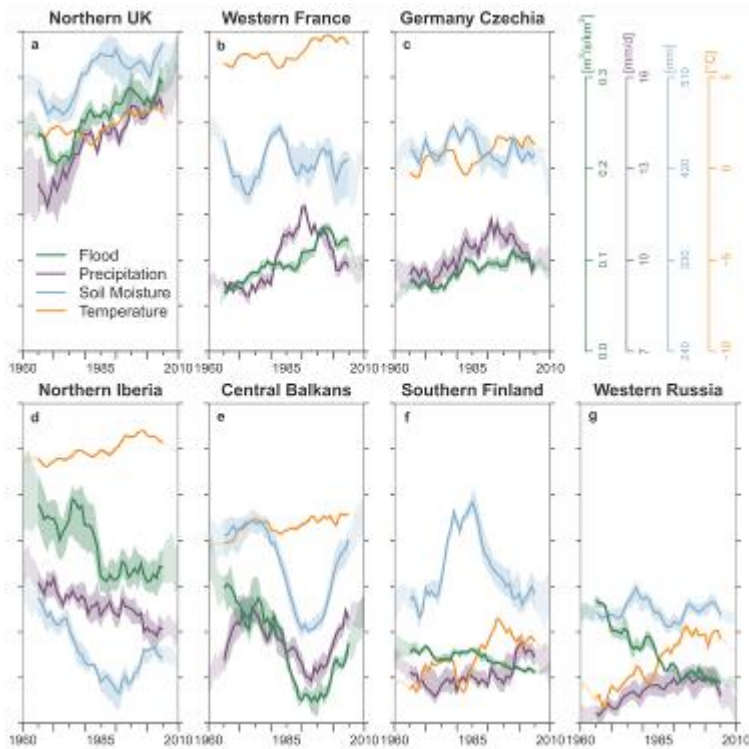


68
 69 **Fig. 1 | Observed regional trends of river flood discharges in Europe (1960–2010).** Blue indicates
 70 increasing flood discharges, red decreasing flood discharges (percentage change per decade of the
 71 mean annual flood discharge). No. 1–3 indicate regions with distinct drivers: [1] northwestern
 72 Europe: increasing rainfall and soil moisture; [2] southern Europe: decreasing rainfall and increasing
 73 evaporation; [3] eastern Europe: decreasing and earlier snowmelt. The trends are based on $n = 2370$
 74 hydrometric stations. For uncertainties see Extended Data Fig. 2b.

75
 76
 77 To interpret these changes we focused on seven hotspots of change, where flood trends are
 78 particularly clear and flood processes are broadly similar⁸ (Extended Data Fig. 2). Because floods
 79 result from the interaction between precipitation, soil moisture and snowmelt, we analyzed the
 80 temporal evolution of these drivers, using air temperature as a surrogate for snowmelt, and compared
 81 them to that of floods (Extended Data Fig. 4 a–g). Depending on the region, some of these drivers
 82 can be more important than others in explaining flood changes⁸.

83
 84 In northern UK, floods predominantly result from winter rains associated with high soil moisture¹⁴
 85 (Extended Data Fig. 4a). The increase in the flood discharges therefore closely follows increases in
 86 winter rainfall and to some degree that of soil moisture (Fig. 2a). This is also shown by statistically
 87 significant positive correlations between the temporal variability of flood discharges and these two
 88 drivers (Spearman rank correlation coefficient $r = 0.70$ and 0.36 , respectively, Table 1). In western
 89 France (Fig. 2b), southern Germany and western Czechia (Fig. 2c), increases in floods are also
 90 associated with increases in rainfall, although the correlation with soil moisture is stronger than in the
 91 UK, reflecting the important role of soil moisture in flood generation during spring and summer¹⁵
 92 (Extended Data Fig. 4 a–c). In northern Iberia (Fig. 2d), decreasing floods are mainly caused by
 93 decreasing winter rainfall, amplified by decreasing soil moisture linked to increasing
 94 evapotranspiration¹⁶. Similarly, in the central Balkans (Fig. 2e), floods have decreased over most of
 95 the study period as a result of decreasing precipitation and soil moisture, but the trend appears to have
 96 reversed in the 1990s. In southern Finland (Fig. 2f) and western Russia (Fig. 2g), floods usually occur
 97 in spring¹⁷, and snowmelt plays an important role. The data show that air temperature has strongly

98 increased (more than 0.5°C per decade) and spring and early summer flood discharges have decreased
 99 ($r = -0.34$ and -0.55 , respectively, Table 1), reflecting shallower snow packs, earlier spring thaw
 100 (Extended Data Fig. 4f-g), and decreasing snowmelt.
 101



102
 103 **Fig. 2 | Long-term temporal evolution of flood discharges and their drivers for seven hotspots**
 104 **in Europe.** (a) Northern UK, (b) Western France (c) Southern Germany and Western Czechia, (d)
 105 Northern Iberia, (e) Central Balkans, (f) Southern Finland, (g) Western Russia. Observed floods
 106 (green), maximum 7-day precipitation (purple), maximum monthly soil moisture (blue), and mean
 107 spring air temperature (orange). Solid lines show the median and shaded bands indicate the spatial
 108 variability within the hotspots (25th and 75th percentile). All data were subjected to a 10-year moving
 109 average filter. Vertical axes are indicated in top right corner.
 110
 111

112 **Table 1 | Spearman's rank correlation coefficient (r) between hotspot medians of the annual**
 113 **series of flood discharge and their drivers.** Confidence bounds of r are given in Extended Data
 114 Table 2b.

	Northern UK	Western France	Germany Czechia	Northern Iberia	Central Balkans	Southern Finland	Western Russia
Precipitation	0.70 **	0.41 *	0.40 *	0.54 **	0.22	0.08	-0.13
Soil Moisture	0.36 *	0.57 **	0.56 **	0.37 *	0.68 **	0.20	0.30
Spring temperature	0.09 †	0.50 ** †	0.04	0.02	-0.29	-0.34	-0.55 **

115 [(**) p -value < 0.001, (*) p -value < 0.01, † Little snow influence on floods. Bold print indicates largest correlation
 116 coefficients in each hotspot.]
 117

118 In northwestern Europe (Fig. 1, region 1), increases in extreme precipitation (Fig. 2a-c; Extended
 119 Data Fig. 5b) are related to the poleward shift of the subpolar jet and associated storm tracks observed
 120 since the 1970s associated with more prevalent positive phases of the North Atlantic Oscillation
 121 (NAO) and polar warming¹⁸. The relationship of NAO variability with polar warming is still debated.
 122 Floods in the northern UK hotspot are closely aligned with increasing precipitation resulting in a
 123 mean flood discharge trend of +6.6% (Extended Data Table 2c).
 124

125 In southern Europe (Fig. 1, region 2), the northward shift of the subtropical jet and associated storm
126 tracks¹⁹ as a result of the expansion of the Hadley cell²⁰ has led to decreasing precipitation, which,
127 together with increasing evapotranspiration¹⁶ related to warmer temperatures, has substantially
128 reduced soil moisture by around 5% per decade (Extended Data Figs. 5b,6b,7b). The combined effect
129 has resulted in decreasing flood discharges in the catchments analyzed here. Small catchments of a
130 few square kilometers are not contained in the data set (the median catchment size of region 2 is about
131 400 km²), as they are usually not monitored or the flood series are too short for trend analyses. In
132 small catchments, local short-duration convective storms with high intensities are more relevant for
133 flood generation than long-duration synoptic storms, which produce floods in medium and large
134 catchments contained in the data²¹. Local convective storms are expected to increase in a warmer
135 climate²², which means that floods in small catchments may have actually increased. Additionally,
136 soil compaction, abandoned terraces and land-cover changes may increase flood discharges in small
137 catchments²³. The difference in catchment size may explain the apparent inconsistency between the
138 occurrence of numerous floods in small catchments in recent years in southern Europe²¹ and the
139 decreasing trend in Fig. 1.

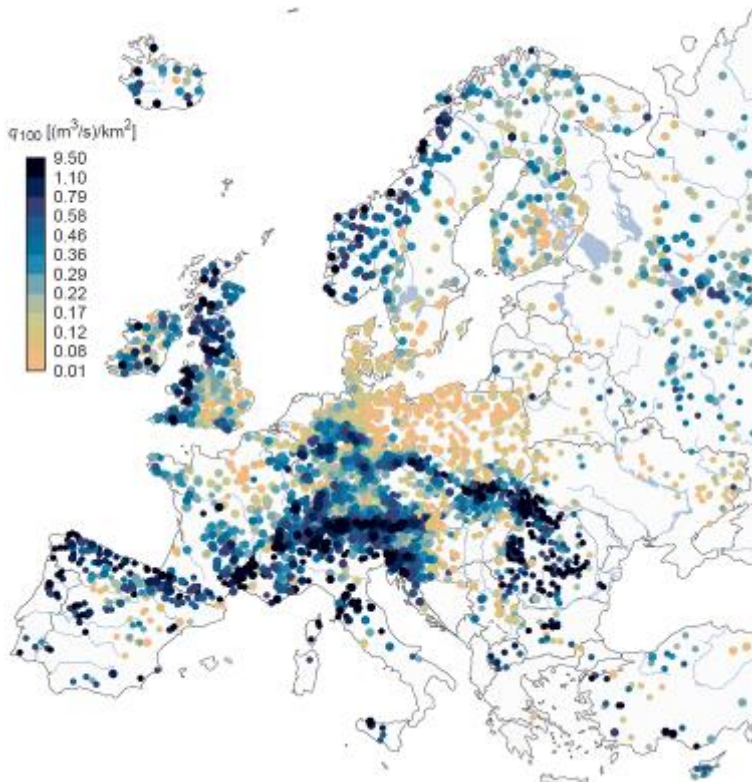
140
141 In all but southern Europe, increases in extreme precipitation (Fig. 2a–c,f,g; Extended Data Fig. 5b)
142 are related to increased atmospheric blocking associated with decreasing pressure differences
143 between Greenland and the Baltic, which has decreased the speed of zonal (west-east) flow and
144 increased the chance of standing planetary waves²⁴. However, it is only in northwestern Europe (Fig.
145 1, region 1), where the increase in extreme precipitation is reflected in increased flood discharges, as
146 winter storms in that region cause winter floods⁸. Further in the east, snowmelt is more relevant for
147 flood generation.

148
149 In eastern Europe, spring air temperature has increased by as much as 1°C per decade (Extended Data
150 Fig. 6b). This has resulted in much less extensive spring snow cover²⁵, a shift of snowfall to rainfall
151 when air temperatures are around zero, shallower snow packs, earlier snowmelt⁸, likely increased
152 infiltration resulting from shallower freezing depths and therefore smaller floods, even though
153 extreme precipitation in summer has increased²⁶. The mean flood trend in the western Russian hotspot
154 is -18.2% (Extended Data Table 2c). Given the colder background temperature (Extended Data Fig.
155 6a) and larger snowpack in northwestern Russia, the increasing temperatures are not yet changing
156 snowmelt patterns, and hence not decreasing floods (Fig. 1).

157
158 While past studies have focused on a few catchments or were clustered around western Europe^{9–11,27},
159 this study provides a continental perspective, which allows for an analysis of climate processes that
160 manifest themselves at larger scales. Isolated local or national scale studies, however, are broadly
161 consistent with our findings.

162
163 Our results have implications for flood risk management in medium and large sized catchments. The
164 trends shown in Fig. 1 are estimates of changes in the mean annual flood. Since mean annual floods
165 and more extreme floods are usually closely correlated²⁸, similar trends could also be expected for
166 the 100-year flood, which is often the key design criterion in flood risk management. In northwest
167 Europe (Fig. 1, region 1), flood discharges per unit catchment area (specific flood discharges) are
168 generally high (Fig. 3). For example, on the west coast of the British-Irish Isles and Norway, the
169 specific 100-year flood discharge during the period 1960-2010 was ~0.9 (m³/s)/km² (Fig. 3), with
170 floods increasing by ~5% per decade. However, in eastern Europe (Fig 1, region 3), specific flood
171 discharges are rather small (Fig. 3), and are likely to become smaller in a changing climate. For
172 example, in the Baltic countries, southern Poland and the Ukraine, the 100-year flood of ~0.1
173 (m³/s)/km² would decrease to ~0.075 (m³/s)/km² if the observed decrease of ~5% per decade persists
174 over the next 50 years. In southern Europe, even if flood discharges decrease in medium and large
175 catchments, discharges are still generally high (Fig. 3), as a result of the proximity to the

176 Mediterranean Sea and associated heavy precipitation events²⁹. Floods in small catchments may
177 actually increase as a result of enhanced convective storms³⁰ and land-use change²³.
178
179



180
181 **Fig. 3 | Specific 100-year floods ((m³/s)/km²) in Europe**, where larger points indicate 90%
182 confidence intervals smaller than 60% of the estimate.
183

184 Increasing flood discharges imply that, the 100-year flood discharge five decades ago, now has a
185 smaller return period than 100 years, i.e. that discharge is likely to be exceeded on average more often
186 than once in 100 years. In northwestern Europe, what was the 100-year flood discharge in 1960 has
187 now typically become a 50- to 80-year flood discharge (Extended Data Fig. 8), which will make flood
188 defense structures less safe. In eastern Europe, the 100-year flood discharge has now become a 125- to
189 250-year flood discharge, which will make structures less economical. While Extended Data Fig. 8,
190 and Fig. 3, do provide a continental overview, they do not replace national-scale and local studies
191 where more detailed information may be available.
192

193 It should be noted that the flood trends observed here do not necessarily extrapolate into the future as
194 they may be related to climate variability rather than persistent changes in time¹¹. Also, the trends
195 depend on the observation period³, so may differ if the observation period is extended. However, the
196 regions with a distinct climatic change signal in observed flood discharges identified here are broadly
197 coherent with the projected flood changes in Europe. Most projections for the end of the 21st century
198 suggest increasing floods in (north)western Europe due to increasing precipitation, and decreasing
199 floods in eastern and northern Europe due to increasing temperatures^{4,5}. This means that changes in
200 flood discharge magnitudes are already underway, which adds credence to those projections and
201 supports the need to account for climate induced changes in flood risk management.
202
203

204 **References:**

- 205 1. IPCC. *Managing the Risks of Extreme Events and Disasters to Advance Climate Change*
206 *Adaptation. A Special Report of Working Groups I and II of the Intergovernmental Panel on*
207 *Climate Change.* (Cambridge University Press, Cambridge, UK and New York, NY, USA, 2012).

- 208 2. EASAC. European Academies' Science Advisory Council Statement; Extreme weather events in
209 Europe - Preparing for climate change adaptation: an update on EASAC's 2013 study. at
210 <<https://easac.eu/publications/details/extreme-weather-events-in-europe/>>
211 3. Hall, J. *et al.* Understanding flood regime changes in Europe: a state of the art assessment. *Hydrol.*
212 *Earth Syst. Sc.* **18**, 2735–2772 (2014).
- 213 4. Kundzewicz, Z. *et al.* Differences in flood hazard projections in Europe-their causes and
214 consequences for decision making. *Hydrol. Sci. J.* **62**, 1–14 (2017).
- 215 5. Thober, S. *et al.* Multi-model ensemble projections of European river floods and high flows at
216 1.5, 2, and 3 degrees global warming. *Environ. Res. Lett.* **13**, 014003 (2018).
- 217 6. UNISDR. *Making Development Sustainable: The Future of Disaster Risk Management. Global*
218 *Assessment Report on Disaster Risk Reduction.* (Geneva, Switzerland: United Nations
219 International Strategy for Disaster Reduction (UNISDR), 2015).
- 220 7. Winsemius, H. C. *et al.* Global drivers of future river flood risk. *Nat. Clim. Chang.* **6**, 381–385
221 (2016).
- 222 8. Blöschl, G. *et al.* Changing climate shifts timing of European floods. *Science* **357**, 588–590
223 (2017).
- 224 9. Mangini, W. *et al.* Detection of trends in magnitude and frequency of flood peaks across Europe.
225 *Hydrol. Sci. J.* **63**, 493–512 (2018).
- 226 10. Berghuijs, W., Aalbers, E., Larsen, J., Trancoso, R. & Woods, R. Recent changes in extreme
227 floods across multiple continents. *Environ. Res. Lett.* **12**, (2017).
- 228 11. Hodgkins, G. A. *et al.* Climate-driven variability in the occurrence of major floods across North
229 America and Europe. *J. Hydrol.* **552**, 704–717 (2017).
- 230 12. Hall, J. *et al.* A European Flood Database: facilitating comprehensive flood research beyond
231 administrative boundaries. *Proc. Int. Assoc. Hydrol. Sci.* **370**, 89–95 (2015).
- 232 13. Sivapalan, M., Blöschl, G., Merz, R. & Gutknecht, D. Linking flood frequency to long-term water
233 balance: Incorporating effects of seasonality. *Water Resour. Res.* **41**, W06012 (2005).
- 234 14. Bayliss, A. C. & Jones, R. C. *Peaks-over-threshold flood database: Summary statistics and*
235 *seasonality. IH Report No. 121.* (Institute of Hydrology, Wallingford, UK, 1993).
- 236 15. Schröter, K., Kunz, M., Elmer, F., Mühr, B. & Merz, B. What made the June 2013 flood in
237 Germany an exceptional event? A hydro-meteorological evaluation. *Hydrol. Earth Syst. Sc.* **19**,
238 309–327 (2015).
- 239 16. Mediero, L., Santillán, D., Garrote, L. & Granados, A. Detection and attribution of trends in
240 magnitude, frequency and timing of floods in Spain. *J. Hydrol.* **517**, 1072–1088 (2014).
- 241 17. Hall, J. & Blöschl, G. Spatial patterns and characteristics of flood seasonality in Europe. *Hydrol.*
242 *Earth Syst. Sc.* **22**, 3883–3901 (2018).
- 243 18. IPCC. *2013: Climate Change 2013: The Physical Science Basis. Contribution of Working Group*
244 *I to the Fifth Assessment Report of the Intergovernmental Panel on Climate Change.* (Cambridge
245 University Press, Cambridge, UK and New York, USA, 2013).
- 246 19. Archer, C. L. & Caldeira, K. Historical trends in the jet streams. *Geophys. Res. Lett.* **35**, (2008).
- 247 20. Kang, S. M. & Lu, J. Expansion of the Hadley cell under global warming: Winter versus summer.
248 *J. Clim.* **25**, 8387–8393 (2012).
- 249 21. Amponsah, W. *et al.* Integrated high-resolution dataset of high-intensity European and
250 Mediterranean flash floods. *Earth Syst. Sci. Data* **10**, 1783–1794 (2018).
- 251 22. Ban, N., Schmidli, J. & Schär, C. Heavy precipitation in a changing climate: Does short-term
252 summer precipitation increase faster? *Geophys. Res. Lett.* **42**, 1165–1172 (2015).
- 253 23. Rogger, M. *et al.* Land-use change impacts on floods at the catchment scale - Challenges and
254 opportunities for future research. *Water Resour. Res.* **53**, 5209–5219 (2017).
- 255 24. Perdigão, R. A. P., Pires, C. A. L. & Hall, J. Synergistic Dynamic Theory of Complex
256 Coevolutionary Systems: Disentangling Nonlinear Spatiotemporal Controls on Precipitation.
257 *arXiv:1611.03403 [math.DS]* (2016).
- 258 25. Estilow, T. W., Young, A. H. & Robinson, D. A. A long-term Northern Hemisphere snow cover
259 extent data record for climate studies and monitoring. *Earth Syst. Sci. Data* **7**, 137–142 (2015).

- 260 26. Frolova, N. L. *et al.* Hydrological hazards in Russia: origin, classification, changes and risk
261 assessment. *Nat. Hazards* **88**, 103–131 (2017).
- 262 27. Mediero, L. *et al.* Identification of coherent flood regions across Europe by using the longest
263 streamflow records. *J. Hydrol.* **528**, 341–360 (2015).
- 264 28. Salinas, J. L., Castellarin, A., Kohnova, S. & Kjeldsen, T. Regional parent flood frequency
265 distributions in Europe-Part 2: Climate and scale controls. *Hydrol. Earth Syst. Sc.* **18**, 4391–4401
266 (2014).
- 267 29. Xoplaki, E., Gonzalez-Rouco, J. F., Luterbacher, J. & Wanner, H. Wet season Mediterranean
268 precipitation variability: influence of large-scale dynamics and trends. *Clim. Dynam.* **23**, 63–78
269 (2004).
- 270 30. Brooks, H. E. Severe thunderstorms and climate change. *Atmos. Res.* **123**, 129–138 (2013).
- 271

272 **Methods**

273 **Data sets**

274 The hydrological data used in this study were obtained from a newly created European Flood
275 Database¹², with subsequent updates, containing data from 3738 hydrometric gauging stations from
276 68 European data sources for the period 1960 to 2010 (Extended Data Table 1). Choice of the study
277 period was guided by a tradeoff between data availability in terms of record length and spatial
278 coverage. The database consists of the highest discharge (daily mean or instantaneous discharge) in
279 each calendar year for each station. For consistency, we chose to analyze the annual maximum flood
280 rather than multiple floods within a year in all stations, as in many areas only annual maxima were
281 available. The stations are located within the domain bounded by 22.25 W – 60.25 E and 34.25 N –
282 71.25 N (Extended Data Fig. 1), and catchment areas range between 5 and 100,000 km².

283
284 The data set was screened for data errors, and catchments that were known, or were identified, to
285 have experienced strong human modifications such as reservoirs that could affect changes in flood
286 discharges were excluded. The screening involved data pre-selection by co-authors and additional
287 visual examination of the flood records in question, analysis of flood seasonality (jumps in timing
288 and large differences to surrounding stations), and examination of the catchment area in google maps.
289 While local human effects on the floods of individual stations cannot be excluded, the focus of this
290 study was on regionally consistent patterns of change where such effects will not be relevant. In a
291 few catchments, the available flood data had been corrected for the effects of reservoirs to represent
292 near natural flood discharge. In a few cases, local reservoirs may influence the data, but this does not
293 affect the regional pattern. The station density is rather uneven (Extended Data Fig. 1b). In southern
294 Europe it is lower as some stations were removed because of reservoir effects. In Italy, reduced record
295 lengths are related to organizational changes of the hydrographic services¹². In eastern Europe the
296 density of available stations is generally lower than in other countries and, again, some stations were
297 removed because of reservoir effects.

298
299 For estimating the flood discharge trends (Fig. 1 and 2, Extended Data Fig. 2 and 8), only stations
300 that satisfied the following three criteria were considered: at least 40 years of data were available
301 during 1960–2010, the record started in 1968 or earlier, and ended in 2002 or later. In the countries
302 with the highest station densities (Austria, Germany, Switzerland), only stations with at least 49 years
303 of data were included in order to obtain a more even spatial distribution across Europe. In Cyprus,
304 Italy and Turkey, stations with at least 30 years of data were included, and in Spain 40 years of data
305 without restrictions to the start and end of the record. This selection resulted in a set of 2370 stations
306 with a median catchment size of 381 km². Sensitivity analyses indicated that the large-scale spatial
307 pattern of increasing and decreasing flood trends across Europe is not influenced by the choice of
308 record length although the trend of individual stations tends to be sensitive to record length, when
309 increasing the required record length by 5 years, the percentage of significantly positive and negative
310 trends (Extended Data Table 2a) changes only slightly from respectively 11.52% and 16.50% to
311 11.04% and 16.95%. In this study we evaluated linear trends of the flood discharges. Alternative
312 models of change (e.g. step changes) could also be tested but are beyond the scope of this study.

313
314 For each hydrometric gauging station, the contributing catchment boundary was derived from the
315 CCM River and Catchment Database³¹. Daily gridded precipitation sum and mean air temperature
316 data from the E-OBS data set (Version 17.0)³² for the period 1960–2010 were used. The data consist
317 of interpolated ground-based observations with a spatial resolution of 0.25°. Monthly gridded soil
318 moisture data from the CPC Soil Moisture data set³³ for the period 1960–2010 were analyzed. The
319 data are model-calculated monthly averaged soil moisture water-height equivalents with a spatial
320 resolution of 0.5°.

321

322

323 **Analysis method**

324 As a first step, we estimated the discharge trend by the Theil-Sen slope estimator^{34,35}. The trend
 325 estimator β is the median slope calculated using the differences of discharge Q over all possible pairs
 326 of years (i and j , $i < j$) within the time series,

$$327 \quad \beta = \text{median} \left(\frac{Q_j - Q_i}{j - i} \right) \quad (1)$$

328 where β has units of m³/s per year, which was plotted as percentage of the mean flood discharge per
 329 decade in Extended Data Fig. 2. The trends were tested for significance by the Mann-Kendall test³⁶
 330 (Extended Data Table 2a). Some false positives, i.e. detected trends where no trend is present, would
 331 be expected because of the large number of stations. The Mann-Kendall test requires the flood
 332 discharges to be temporally independent. We therefore tested whether lag 1 autocorrelation exists in
 333 the residuals from the trends. 92% of the stations did not exhibit significant lag 1 autocorrelation at
 334 the 5% level, suggesting that the Mann-Kendall test is applicable. To identify regional spatial patterns
 335 within Europe, β was spatially interpolated using the *autoKrige* function (automatic kriging) of the R
 336 *automap* package³⁷. The derived trend patterns are plotted in Fig. 1 and in the background of Extended
 337 Data Fig. 2a. The uncertainty of the estimated trends at the stations was estimated by bootstrapping⁴⁰
 338 and is shown as points in Extended Data Fig. 2b. The uncertainty of the regional trends was estimated
 339 as the block kriging standard deviation (kriging error) using the *autoKrige* function and is shown in
 340 the background of Extended Data Fig. 2b. The variogram estimated by the function is

$$341 \quad \gamma(h) = c_0 + c_1 \left(1 - \frac{1}{2^{v-1}\Gamma(v)} \left(\frac{h}{r} \right)^v K_v \left(\frac{h}{r} \right) \right) \quad (2)$$

342 where h is lag, $c_0 = 10.061$ (%/decade)², $c_1 = 57.708$ (%/decade)², $r = 2394.4$ km, $v = 0.2$ and K_v is
 343 the modified Bessel function of the second kind. We used block kriging rather than ordinary kriging
 344 as we are interested in the uncertainty of the regional estimate rather than that of the local estimate.
 345 The uncertainty is evaluated at a 200 x 200 km block size which is the scale at which we suggest Fig.
 346 1 and Extended Data Fig. 2a to be read.

347
 348 In order to evaluate the robustness of the spatial trend patterns we repeated the interpolation, however,
 349 only using stations with significant trends (Extended Data Fig. 3a). The overall pattern is similar to
 350 that of the interpolation using all stations (Extended Data Fig. 2a). Additionally, we repeated the
 351 interpolation but only using randomly selected stations with distances from each other larger than 50
 352 km to examine the effect of spatial correlations on the trends (Extended Data Fig. 3b). Again, the
 353 patterns are similar.

354
 355 As a second step, we selected rectangular areas or hotspots of change based on similarity of discharge
 356 trends and average flood timing as a proxy for flood processes (Extended Data Fig. 2, Extended Data
 357 Table 2c). We standardized the flood series of individual stations to zero mean and unit variance to
 358 make flood changes within hotspots comparable,

$$359 \quad Q_{i,k}^0 = \frac{Q_{i,k} - \mu_{Q_k}}{\sigma_{Q_k}} \quad (3)$$

360 where μ_{Q_k} and σ_{Q_k} are the mean and the standard deviation of station k , respectively. To compare
 361 results between the hotspots we denormalised the flood series of each hotspot h by the mean specific
 362 flood discharge μ_h ((m³/s)/km²) over all years, and the square root σ_h of the mean temporal variance,

$$363 \quad Q_{i,k}^* = \sigma_h Q_{i,k}^0 + \mu_h \quad (4)$$

364 and estimated the long-term evolution in flood discharge with a centered 10-year moving averaging
 365 window. We plotted the median of these series within each hotspot (solid lines) and 25th and 75th
 366 percentiles of all stations in that hotspot (shaded bands) in Fig. 2. Additionally, the original local
 367 flood discharges were tested for significance of a general trend in each hotspot by the Regional Mann-
 368 Kendall test³⁸ (Extended Data Table 2c). Names of hotspots are only indicative and do not correspond
 369 to any exactly defined geographic area.

370

371 To investigate rain-induced effects on flood changes, we identified for each grid point of the E-OBS
 372 dataset the 7-day period with maximum precipitation in each calendar year (with at least 30 years of
 373 annual data available). Increases of spring temperatures around or below the freezing point are
 374 considered a proxy for snow accumulation, melt and the transition from snowfall to rainfall. To
 375 understand the effect of these snowmelt processes on flood discharge, we calculated mean air
 376 temperature from January to April. When soil moisture is high, even small rainstorms may produce
 377 floods. To understand the effect of high soil moisture on floods, we identified for each grid point of
 378 the CPC Soil Moisture dataset the highest monthly soil moisture in each calendar year. We repeated
 379 the trend analyses for annual maximum precipitation, spring temperature, and annual maximum
 380 monthly soil moisture (Extended Data Fig. 5–7) on a 0.5° grid.

382 In the hotspot analyses, the time series for these three climate variables were extracted based on their
 383 location within the catchment boundaries (or within a buffer distance for small areas), from which
 384 Spearman’s rank correlation coefficients (r) with the spatial medians of the original flood discharge
 385 series were calculated (Table 1). Confidence bounds at the 90% confidence level of r were estimated
 386 by stochastic block bootstrapping (*boot* package of R, random block size geometrically distributed
 387 with mean of 5 years) and are given in Extended Data Table 2b. The long-term evolution of the three
 388 climate variables were calculated and plotted in a similar fashion as those of the floods in Fig. 2.

390 We also analysed changes in the timing of the climate indices and floods as proxies for changing
 391 flood processes using previously established methods⁸ (Extended Data Fig. 4). The timing is used to
 392 interpret the process drivers of flood discharge changes. For Extended Data Fig. 4a, b, d the snow
 393 melt index is not shown, as it is of little relevance for flooding⁸.

395 To evaluate the relevance of the observed flood changes for flood management, the 100-year flood
 396 (Q_{100}) was estimated for each station using a Generalised extreme value (GEV) distribution

$$397 \quad Q_T = \xi + \frac{\eta}{\kappa} \cdot \left[1 - (-\ln(1 - 1/T))^\kappa \right] \quad (5)$$

398 where Q_T is the T -year flood discharge. The parameters ξ , η and κ were estimated from the flood
 399 discharge series by Bayesian inference through an MCMC algorithm³⁹. Non-informative uniform
 400 prior distributions were used for ξ and $\log(\eta)$, while a normal distribution consistent with the
 401 geophysical prior⁴¹ were used for κ . 4000 parameter samples were drawn from the posterior
 402 distributions from which 4000 100-year floods were calculated for each station by Eq. (5). The
 403 median and the relative width of the 90% credible intervals are shown in Fig. 3. For comparability of
 404 the 100-year flood in catchments of different sizes, flood discharges per unit catchment area (specific
 405 flood discharges; $q_{100}=Q_{100}/A$, where A is catchment area) are shown.

407 If flood discharges change over time, the return period T may also change, e.g., the 100-year flood
 408 may become the 10-year flood if the flood discharges increase. Change in return period was therefore
 409 estimated by allowing the parameter ξ in Eq. (5) to change with time t as

$$410 \quad \xi = a + b \cdot t \quad (6)$$

411 where the posterior distributions of a , b , η and κ were estimated from the flood discharge series by
 412 Bayesian inference through the same MCMC algorithm³⁹, using non-informative uniform prior
 413 distributions for a and b . More complex models than (6) were excluded because, for most of the
 414 stations, they did not outperform (6) based on the WAIC information criterion⁴². 4000 parameter
 415 samples were drawn from the posterior distributions from which 4000 100-year floods in 1960 were
 416 calculated for each station by Eqs. (5) and (6) with $t = 1960$. The changed return period in 2010 of
 417 these 4000 flood peaks were computed by inverting Eq. (5) and by Eq. (6) with $t = 2010$. Finally, the
 418 median of the 4000 return periods was used as the 2010 return period of the 100-year flood discharge
 419 in 1960. Those stations where the 5th and the 95th percentiles of the uncertainty distribution agreed in

420 the sign of change, were plotted as large points in Extended Data Fig. 8 while those where this was
421 not the case were plotted as smaller points to indicate the uncertainty involved in the estimation.
422

423 To identify large-scale spatial patterns, the logarithms of the 2010 return periods of the 100-year flood
424 discharge in 1960 were spatially interpolated using the *autoKrige* function³⁷ (Extended Data Fig. 8).
425 For estimating the stationary 100-year specific flood discharge q_{100} (Eq. (5), Fig. 3), less stringent
426 selection criteria (at least 30 years of data) than in all the other analyses were used as it can be
427 estimated more robustly than trends and changes in the return period, which resulted in 3738 stations
428 (Extended Data Fig. 1a).
429

430 In this paper we have analyzed flood discharge trends. The flood data set is freely available and can
431 be used for a wide range of analyses.
432

433

434 **Data Availability**

435 The flood discharge data from the data holders/sources listed in Extended Data Table 1 that were used in this
436 paper can be downloaded from Zenodo. The precipitation and temperature data from the E-OBS dataset can
437 be downloaded from www.ecad.eu/download/ensembles/ensembles.php. The CPC soil moisture data can be
438 downloaded from www.esrl.noaa.gov/psd.
439

440

440 **Code Availability**

441 The code for the trend and extreme value analyses can be downloaded from GitHub.
442

443

443 **References Methods**

- 444 31. Vogt, J. *et al.* A pan-European River and Catchment Database. European Commission, Joint
445 Research Centre (2007).
- 446 32. Haylock, M. *et al.* A European daily high-resolution gridded data set of surface temperature and
447 precipitation for 1950-2006. *J. Geophys. Res.* **113**, (2008).
- 448 33. Van den Dool, H., Huang, J. & Fan, Y. Performance and analysis of the constructed analogue
449 method applied to US soil moisture over 1981-2001. *J. Geophys. Res.* **108**, (2003).
- 450 34. Sen, P. K. Estimates of the Regression Coefficient Based on Kendall's Tau. *J. Am. Stat. Assoc.*
451 **63**, 1379–1389 (1968).
- 452 35. Theil, H. A Rank-invariant Method of Linear and Polynomial Regression Analysis, Part 1. *Proc.*
453 *R. Neth. Acad. Sci.* **53**, 386–392 (1950).
- 454 36. Mann, H. B. Nonparametric tests against trend. *Econometrica: Journal of the Econometric*
455 *Society*, 245-259 (1945).
- 456 37. Hiemstra, P. H., Pebesma, E. J., Twenhöfel, C. J. & Heuvelink, G. B. Real-time automatic
457 interpolation of ambient gamma dose rates from the Dutch radioactivity monitoring network.
458 *Comput. Geosci.* **35**, 1711–1721 (2009).
- 459 38. Helsel, D. R. & Frans, L. M. Regional Kendall Test for Trend. *Environ. Sci. Technol.* **40**, 4066–
460 4073 (2006).
- 461 39. Renard, B., Lang, M. & Bois, P. Statistical analysis of extreme events in a non-stationary context
462 via a Bayesian framework: case study with peak-over-threshold data. *Stoch. Env. Res. Risk A.* **21**,
463 97–112 (2006).
- 464 40. Wilcox, R. A note on the Theil - Sen regression estimator when the regressor is random and the
465 error term is heteroscedastic. *Biometrical Journal: Journal of Mathematical Methods in*
466 *Biosciences*, 40(3), 261-268 (1998).
- 467 41. Martins, E. S., & Stedinger, J. R. Generalized maximum-likelihood generalized extreme-value
468 quantile estimators for hydrologic data. *Water Resources Research*, 36(3), 737-744 . (2000).
- 469 42. Watanabe, S. (2010). Asymptotic equivalence of Bayes cross validation and widely applicable
470 information criterion in singular learning theory. *Journal of Machine Learning Research*, 11,
471 3571-3594.

472
473
474
475
476
477
478
479
480
481
482
483
484
485
486
487
488
489
490
491
492
493
494
495
496
497
498
499
500
501

ACKNOWLEDGEMENTS

Supported by the ERC Advanced Grant “FloodChange” project (no. 291152), the Horizon 2020 ETN “System Risk” project (no 676027), the DFG “SPATE” project (FOR 2416), the FWF “SPATE” project (I 3174), and a Russian Foundation for Basic Research (RFBR) project (no. 17-05-41030 rgo_a). The data analysis was performed in R using the supporting packages *automap*, *boot*, *lattice*, *maptools*, *ncdf4*, *plyr*, *raster*, *RColorBrewer*, *rgdal* and *rworldmap*. The authors also acknowledge the involvement in the data screening process of C. Álvaro Díaz, I. Borzì, E. Diamantini, K. Jeneiová, M. Kupfersberger, S. Mallucci and S. Persiano during their stays at the Vienna University of Technology. We thank L. Gaál and D. Rosbjerg for contacting Finnish and Danish data holders, respectively; B. Renard (France), W. Rigott (South Tyrol, Italy), G. Lindström (Sweden) and P. Burlando (Switzerland) for assistance in preparing and/or providing data or metadata from their respective regions. We acknowledge all flood data providers listed in Extended Data Table 1.

Author contributions

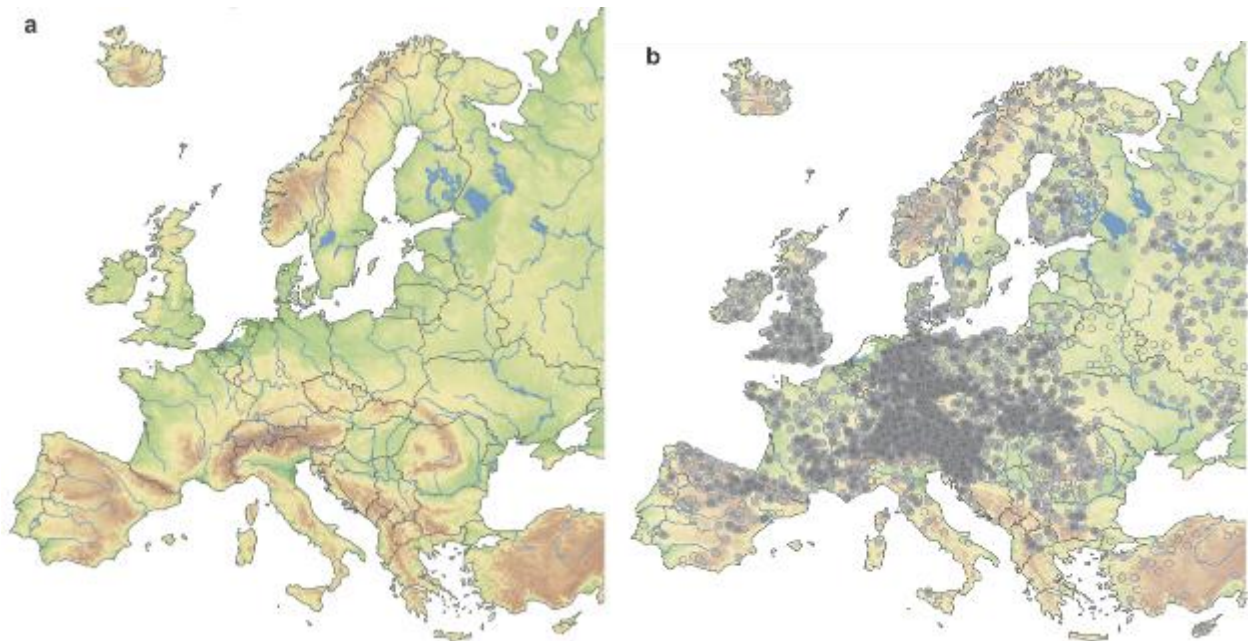
G.B. and J.H. designed the study and wrote the first draft of the paper. G.B. initiated the study. J.H. collated the database with the help of most of the co-authors, and conducted the analyses. A.V. conducted the MCMC analysis. G.B., J.H., A.V., R.P., J.P. and B.M. interpreted the results in the context of underlying geophysical mechanisms. J.P. compiled the catchment boundaries. D.L. contributed to the statistical analysis. M.B., I.Č., A.K., S.K., O.L., M.M.-G., R.M., P.M., I.R., J.L.S., J.S. and N.Ž. interpreted the results in central Europe. G.T.A., A.B., O.B., M.B., A.C., G.B.C., P.C., D.G., A.M., L.M., M.Š., E.V. and K.Z. interpreted the results in southern Europe. B.A., J.J.K. and D.W. interpreted the results in northern Europe. J.H., S.H., T.R.K., N.M., C.M. and E.S. interpreted the results in western Europe. N.F., L.G., A.G., M.K., M.O. and V.O. interpreted the results in eastern Europe. All authors contributed to framing and revising the paper.

Competing interests The authors declare no competing interests.

Correspondence should be addressed to G.B. (bloeschl@hydro.tuwien.ac.at)

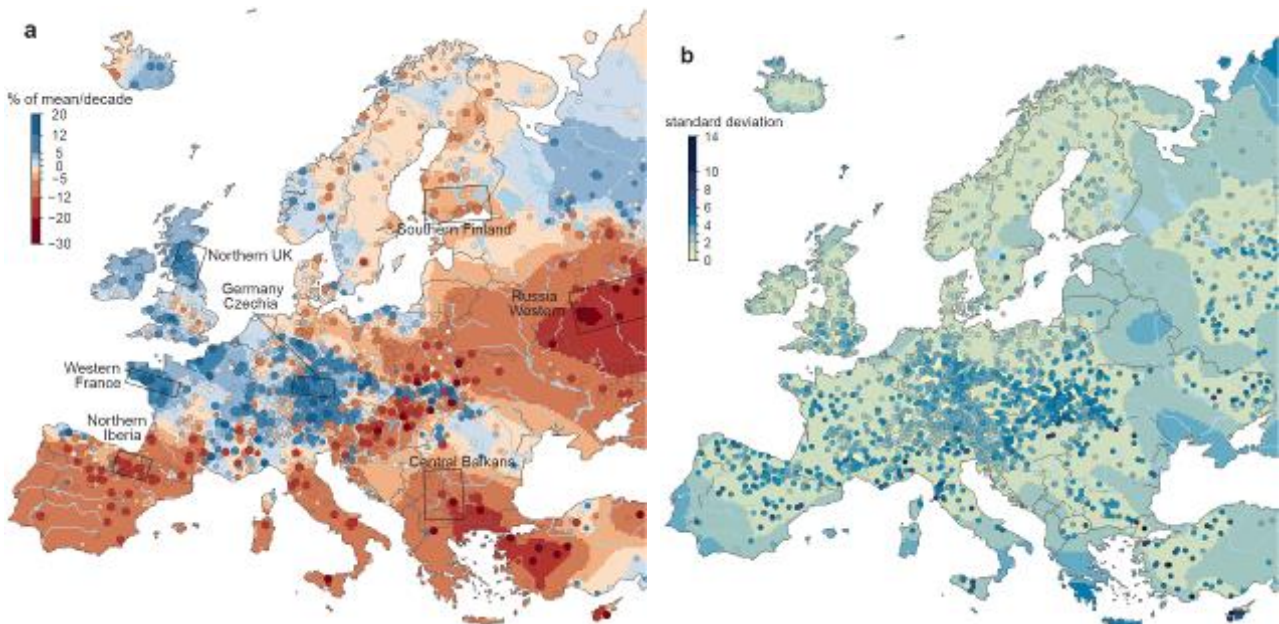
502 **Extended Data display items**

503



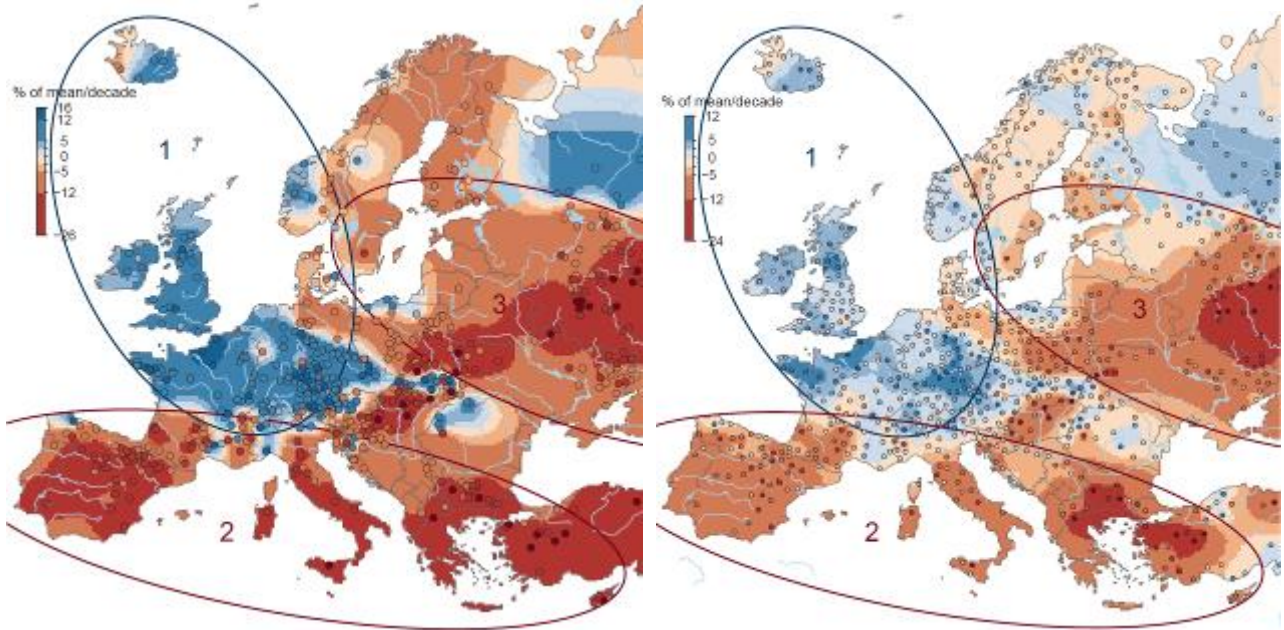
504
505
506
507
508
509
510

Extended Data Figure 1 | Map of European study area. (a) Elevation, main rivers and lakes and (b) location of the hydrometric stations analyzed. Open and full circles indicate stations with ≥ 30 years ($n = 3738$) and ≥ 40 years ($n = 2835$) of flood discharge data, respectively.

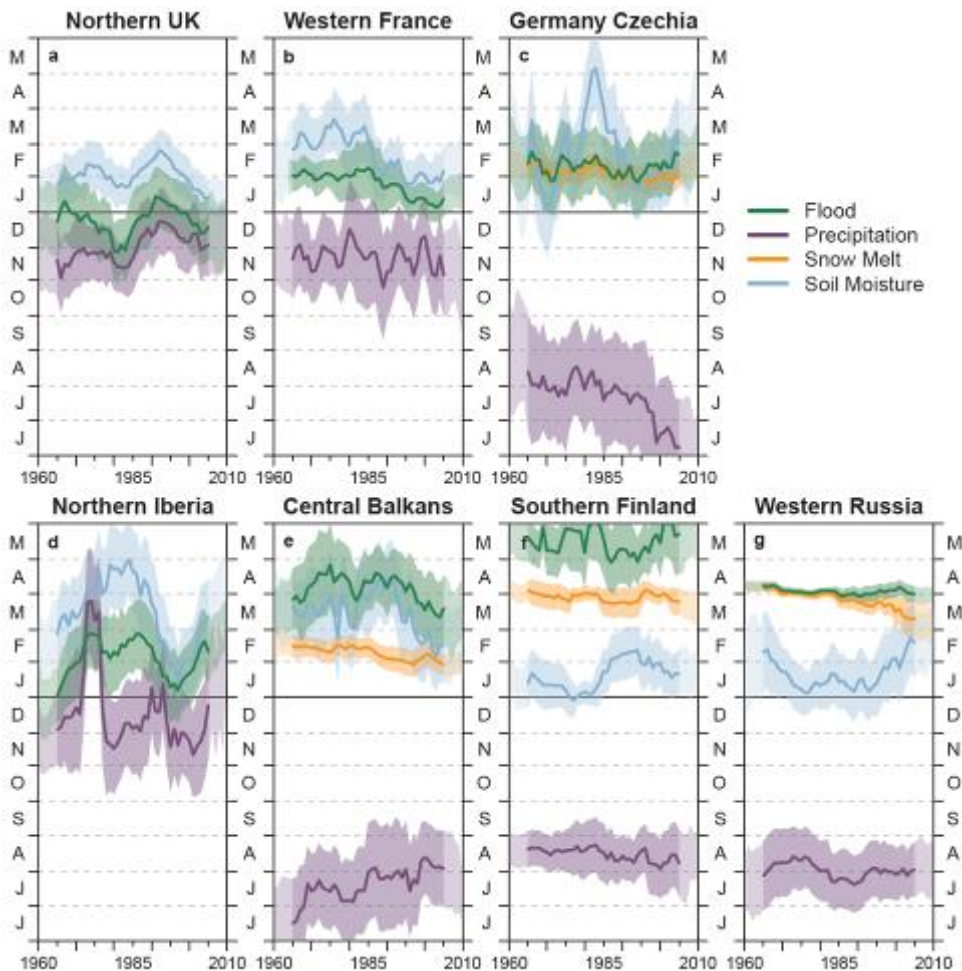


511
512
513
514
515
516
517
518

Extended Data Figure 2 | Observed trends of river flood discharges in Europe (1960–2010). (a) Points show local trends ($n = 2370$), where larger points indicate statistically significant trends ($\alpha = 0.1$). Background pattern represents regional trend. Blue indicates increasing flood discharges, red decreasing flood discharges. Rectangles indicate hotspot areas as in Fig. 2, Extended Data Fig. 3 and Extended Data Table 2c. (b) Uncertainties of the trends in terms of standard deviation. Points show local uncertainties. Background pattern represents regional uncertainties at the scale of a block size of 200 x 200 km. Units of both panels are % of mean/decade.

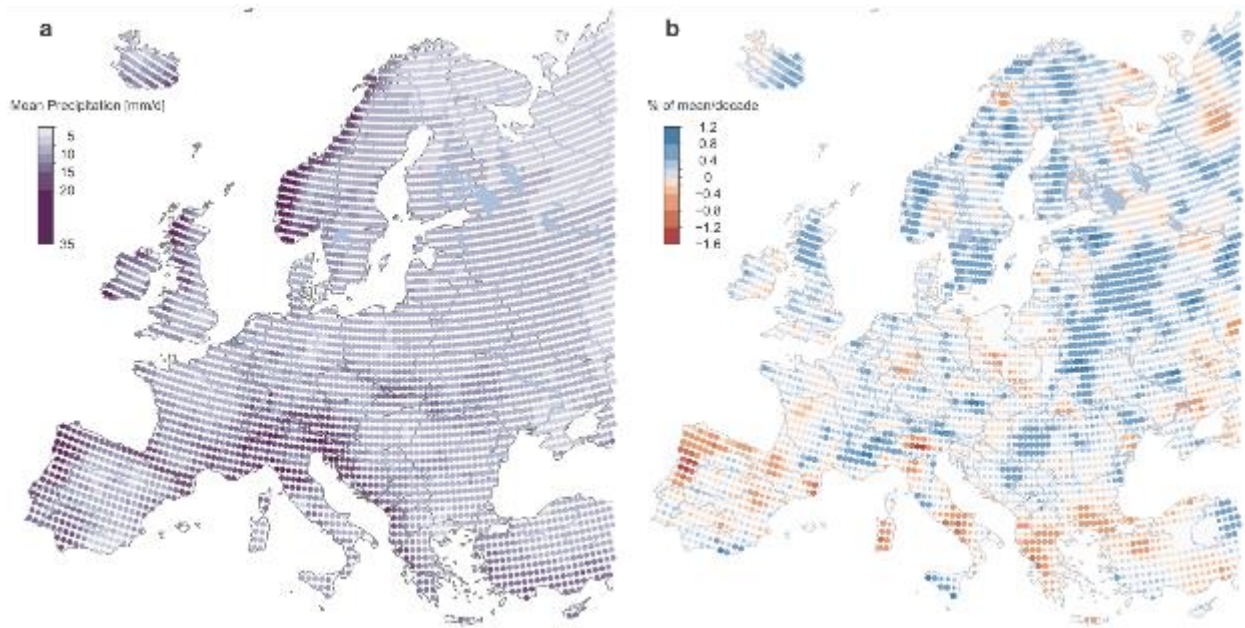


519
 520 **Extended Data Figure 3 | Flood trends as in Fig. 1 and Extended Data Figure 2, but using fewer stations.** (a)
 521 Only stations with significant trends are used (n = 664). (b) Only stations with distances from each other
 522 larger than 50 km are used (n = 745).
 523
 524
 525



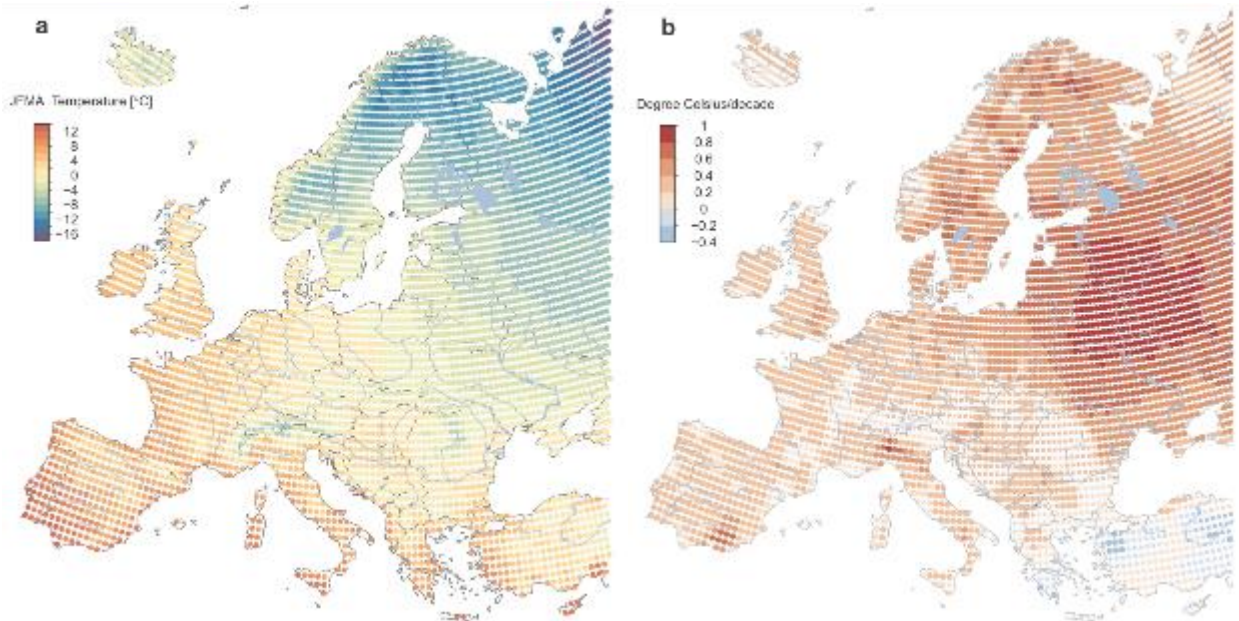
526
527
528
529
530
531
532
533
534

Extended Data Figure 4 | Long-term temporal evolution of timing of floods and their drivers for seven hotspots in Europe. (a) Northern UK, (b) Western France, (c) Southern Germany and Western Czechia, (d) Northern Iberia, (e) Central Balkans, (f) Southern Finland, (g) Western Russia. Timing of observed floods (green), 7-day maximum precipitation (purple), snowmelt index (orange), and maximum monthly soil moisture (blue). Lines show median timing and shaded bands indicate variability of timing within the year (± 0.5 circular standard deviations). All data were subjected to a circular 10-year moving average filter. Vertical axes show month of the year (June to May).

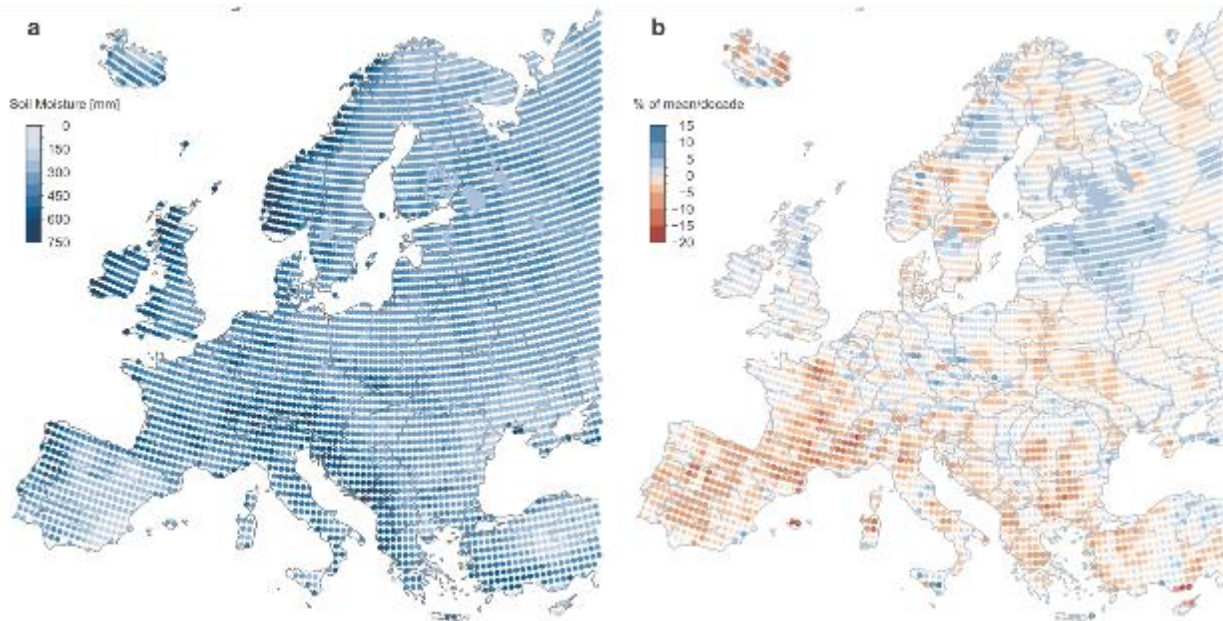


535
 536
 537
 538
 539
 540
 541

Extended Data Figure 5 | 7-day maximum precipitation (1960–2010). (a) Long-term mean (mm/d); (b) trends in precipitation (% of mean per decade), where larger points indicate statistically significant trends ($\alpha = 0.1$); blue indicates increasing precipitation, red decreasing precipitation.

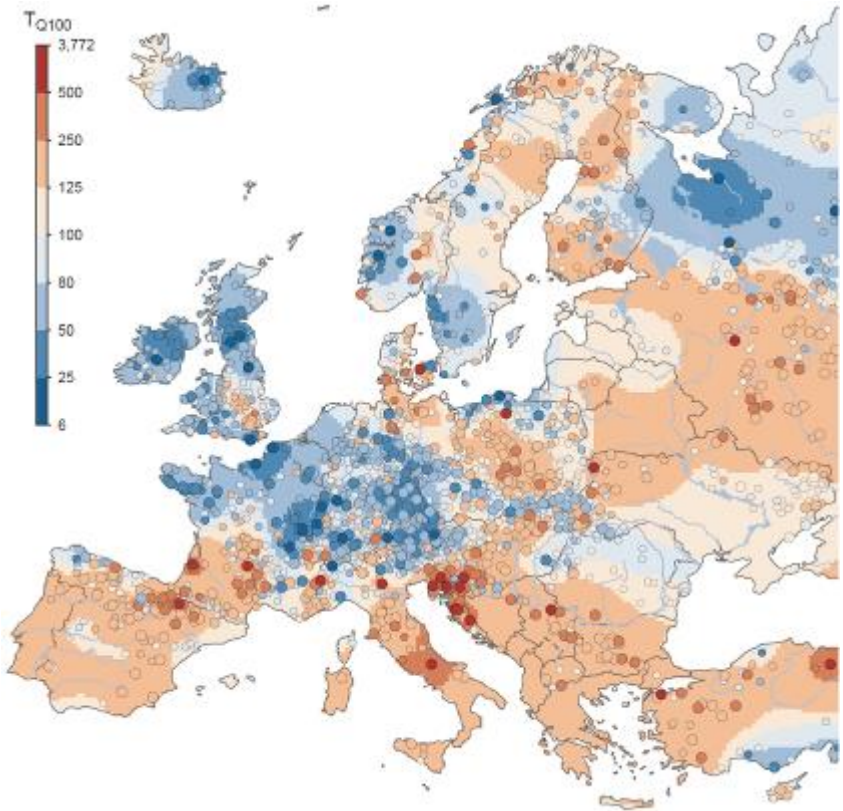


543
544 **Extended Data Figure 6 | Spring (January to April) mean air temperatures (1960–2010).** (a) Long-term
545 mean (°C); (b) trends in temperatures (°C per decade), where larger points indicate statistically significant trends
546 ($\alpha = 0.1$); red indicates increasing temperature, blue decreasing temperature.
547



549
550
551
552
553

Extended Data Figure 7 | Annual maximum monthly soil moisture (1960–2010). (a) long-term mean (mm); (b) trends in maximum soil moisture (% of mean per decade), where larger points indicate statistically significant trends ($\alpha = 0.1$); blue indicates increasing soil moisture, red decreasing soil moisture.



554
 555
 556
 557
 558
 559
 560
 561
 562

Extended Data Figure 8 | Estimated return period in 2010 of the discharge that was the 100-year flood in 1960. Points show local return periods ($n = 2370$), where larger points indicate agreement of the 5th and the 95th percentiles of the uncertainty distribution in the sign of change. Background pattern represents regional return periods. Blue indicates lower return periods representing increasing flood discharges, red indicates higher return periods representing decreasing flood discharges. This figure provides a continental overview, and does not replace national-scale and local studies where more detailed information may be available.

Extended Data Table 1 | Data Sources contained in the European Flood Research Database.

Country/Project	Data Holder/Source/Project information
Albania	National Hydro-Meteorological Service Albania, Institute of GeoSciences, Energy, Water and Environment (IGEWE)
Austria	Hydrographic Services of Austria (HZB)
Bosnia and Herzegovina	Hydrological Yearbooks of the former Republic of Yugoslavia
Bulgaria	Meteorological Yearbooks of the Rivers in Bulgaria, National Institute of Meteorology and Hydrology
Croatia	Meteorological and Hydrological Service of Croatia
Czechia	Czech Hydrometeorological Institute
Denmark	Danish Centre for Environment and Energy (DCE)
Estonia	Estonian Environment Agency
EWA	European Water Archive (EWA)
Finland	Finnish Environment Institute, Open information/Hydrology/Discharge, Source: SYKE
France	HYDRO database, French Ministry of Ecology, Sustainable Development and Energy
Germany	Federal Waterways and Shipping Administration (WSV)
Germany, Baden-Wuerttemberg	Ministry for the Environment, Climate and Energy of the Federal State of Baden-Wuerttemberg (LUBW)
Germany, Bavaria	Flood Information Centre, Bavarian Environment Agency, Munich (LfU)
Germany, Brandenburg	Ministry of Rural Development, Environment and Agriculture of the Federal State of Brandenburg (MLUL)
Germany, Hesse	Hessian Agency for Nature Conservation, Environment and Geology (HLNUG)
Germany, Lower Saxony	Lower Saxony Water Management, Coastal Defence and Nature Conservation Agency (NLWKN)
Germany, Mecklenburg-Western Pomerania	State Office of Environment, Nature Protection and Geology of Mecklenburg-Western Pomerania (LUNG)
Germany, North Rhine-Westphalia	State Agency for Nature, Environment and Consumer Protection (LANUV)
Germany, Rhineland-Palatinate	State Office for the Environment, Water Management and Commerce Inspectorate Rhineland-Palatinate (LUWG)
Germany, Saarland	The Saarland State Office for Environmental and Labour Protection (LUA)
Germany, Saxony	Saxon State Agency for Environment, Agriculture and Geology (LfULG)
Germany, Saxony-Anhalt	State Agency for Flood Defence and Water Management of Saxony-Anhalt (LHW)
Germany, Schleswig-Holstein	Schleswig-Holstein Agency for Coastal Defence, National Park and Marine Conservation (LKN.SH)
Germany, Thuringia	Thuringian Regional Office for the Environment and Geology (TLUG)
GRDC	The Global Runoff Data Centre, Koblenz, Germany
Greece	National Data Bank of Hydrological & Meteorological Information (NDBHMI)
Hungary	General Directorate of Water Management, Hungary
HYDRATE	EU-FP7 HYDRATE Project data base: Hydrometeorological Data Resources and Technology for Effective Flash Flood Forecasting
Iceland	Icelandic Meteorological Office, Hydrological Database, No. 2013-10-27/01
Ireland	Irish Environmental Protection Agency (EPA)
Ireland	Office of Public Works (OPW)
Italy	CUBIST database, former SIMN (Servizio Idrografico e Mareografico Nazionale)
Italy	National Research Council - Consiglio Nazionale delle Ricerche (CNR)
Italy	ENEL (Ente Nazionale per l'Energia Elettrica)
Italy	AdBPo (Autorità di Bacino del Fiume Po)
Italy	IRPI (Istituto di Ricerca per la Protezione Idrogeologica)
Italy	ISPRA (Istituto Superiore per la Protezione e la Ricerca Ambientale)
Italy, Emilia-Romagna Region	ARPA (Agenzia Regionale per la Protezione dell' Ambiente) Emilia-Romagna
Italy, Piedmont Region	ARPA Piemonte
Italy, Lazio Region	Ufficio Idrografico e Mareografico di Roma - Regione Lazio
Italy, Sicily Region	Osservatorio delle Acque della Regione Siciliana
Italy, South Tyrol Region	Hydrographic Office, Autonomous Province of Bolzano
Italy, Trentino Region	Dipartimento Protezione Civile, Provincia Autonoma di Trento
Italy, Umbria Region	Ufficio Idrografico - Regione Umbria
Italy, Veneto Region	ARPA Veneto
Latvia	Latvian Environment, Geology and Meteorology Centre, State Ltd.
Lithuania	Lithuanian Hydrometeorological Service
Macedonia	Macedonian Hydrometeorological Service
Netherlands	Rijkswaterstaat - Dutch Ministry of Infrastructure and the Environment
Norway	Norwegian Water Resources and Energy Directorate - Norges vassdrags- og energidirektorat (NVE)
Poland	Institute of Meteorology and Water Management National Research Institute (IMGW-PIB)
Portugal	Portuguese Environmental Agency - Agência Portuguesa do Ambiente, National Information System for Water Resources of Portugal (SNIRH)
Romania	National Institute of Hydrology and Water Management - NIHWM
Russia	The main hydrological characteristics, 1963-1970, 1971-75, 1975-1980, 1980-2000
Russia	Ministry of Natural Resources and Ecology of the Russian Federation, State Hydrological Institute
Russia	State Water Cadastre, 1985-2010, State Hydrological Institute, Lomonosov Moscow State University
Russia	Automated information system of state water bodies monitoring (AIS GMVO), Federal Agency for Water Resources
Serbia	Republic Hydrometeorological Service of Serbia (RHSS), Hydrological Yearbooks of Surface Water, Belgrade
Slovakia	Slovak Hydrometeorological Institute (SHMI)
Slovenia	Slovenian Environment Agency (ARSO)
Spain	Centre for Hydrographic Studies (Centro de Estudios Hidrográficos) of CEDEX, Spain
Sweden	Swedish Meteorological and Hydrological Institute (SMHI)
Switzerland	Federal Office for the Environment (FOEN) / (BAFU)
Turkey	General Directorate of Electrical Power Resources Survey and Development Administration (EIE), Turkey
Ukraine	Hydrological Department, Ukrainian Hydrometeorological Institute (UHMI)
Ukraine	Hydrometeorological Institute, Odessa State Environmental University (OSENU)
United Kingdom	UK National River Flow Archive (NRFA)

567
568

Extended Data Table 2a | Number of stations with positive and negative flood discharge trends. Regions according to Fig. 1.

		Positive Trend	Negative Trend	All
Europe	Significant $\alpha=0.1$	273 (11.52%)	391 (16.50%)	664 (28.02%)
	Not Significant	833 (35.15%)	837 (35.31%)	1706 (71.98%)*
	All	1106 (46.67%)	1228 (51.81%)	2370*
Region 1: North-western Europe	Significant $\alpha=0.1$	182 (20.34%)	27 (3.01%)	209 (23.35%)
	Not Significant	435 (48.60%)	240 (26.82%)	686 (76.65%)*
	All	617 (68.94%)	267 (29.83%)	895*
Region 2: Southern Europe	Significant $\alpha=0.1$	13 (2.84%)	142 (31.00%)	155 (33.84%)
	Not Significant	96 (20.96%)	169 (42.80%)	303 (66.16%)*
	All	109 (23.80%)	338 (73.80%)	458*
Region 3: Eastern Europe	Significant $\alpha=0.1$	5 (1.77%)	115 (40.78%)	120 (42.55%)
	Not Significant	54 (19.15%)	104 (36.88%)	162 (57.45%)*
	All	59 (20.92%)	219 (77.66%)	282*

[*stations with no trend included]

569
570
571
572
573
574

Extended Data Table 2b | Estimates and 90% confidence bounds (in brackets) of Spearman's rank correlation coefficient (r) between hotspot medians of the annual series of flood discharge and their drivers.

	Northern UK	Western France	Germany Czechia	Northern Iberia	Central Balkans	Southern Finland	Western Russia
Precipitation	0.70** (0.57, 0.76)	0.41* (0.15, 0.64)	0.40* (0.24, 0.56)	0.54** (0.39, 0.68)	0.22 (-0.11, 0.49)	0.08 (-0.11, 0.28)	-0.13 (-0.4, 0.18)
Soil Moisture	0.36* (-0.01, 0.66)	0.57** (0.39, 0.71)	0.56** (0.41, 0.68)	0.37* (0.12, 0.55)	0.68** (0.50, 0.76)	0.20 (0.01, 0.4)	0.30 (0.07, 0.49)
Spring temperature	0.09 (-0.15, 0.25)	0.5** (0.33, 0.63)	0.04 (-0.19, 0.23)	0.02 (-0.23, 0.32)	-0.29 (-0.44, -0.12)	-0.34 (-0.49, -0.15)	-0.55** (-0.7, -0.3)

[(**) p -value < 0.001, (*) p -value < 0.01]

575
576
577
578
579
580

Extended Data Table 2c | Flood discharge trends for selected hotspots (as % of station mean per decade). The significance level of the general hotspot trends is given according to the Regional Mann-Kendall test³⁸ with significance level α .

Hotspot Name	No. of Stations	Minimum trend	Maximum trend	Mean hotspot trend	Significance
Northern UK	15	2.9	12.5	6.6	$\alpha < 0.01$
Western France	16	5.9	17.6	9.7	$\alpha < 0.01$
Germany Czechia	47	1.6	17.8	8.0	$\alpha < 0.01$
Northern Iberia	34	-18.3	3.8	-8.3	$\alpha < 0.01$
Central Balkans	15	-17.6	-0.1	-8.4	$\alpha < 0.01$
Southern Finland	15	-10.0	-2.1	-5.2	$\alpha < 0.01$
Western Russia	21	-28.8	-8.3	-18.2	$\alpha < 0.01$

581
582
583
584